ELSEVIER

Journal of Alloys and Compounds 218 (1995) 90–94

Journal of ALLOYS AND COMPOUNDS

Crystal structure, magnetic and electrical properties of the new ternary stannide Ce_2Ni_2Sn

F. Fourgeot, B. Chevalier *, P. Gravereau, L. Fournès, J. Etourneau

Laboratoire de Chimie du Solide du CNRS, Université Bordeaux I, 351 cours de la Libération, 33405 Talence, France

Received 4 August 1994

Abstract

The crystal structure of Ce_2Ni_2Sn has been investigated by single-crystal X-ray diffractometry. This stannide adopts an orthorhombic structure related to the W_2CoB_2 type (space group, *Immm*), the unit cell parameters being $a = 0.439\ 36(9)$ nm, $b = 0.573\ 96(9)$ nm and $c = 0.859\ 67(13)$ nm. The magnetization and electrical resistivity measurements reveal that Ce_2Ni_2Sn orders antiferromagnetically at $T_N = 4.7$ K. This study shows that the Kondo effect plays an important role in the physical properties of Ce_2Ni_2Sn.

Keywords: Cerium stannides; Crystal structure; Antiferromagnetism; Kondo effect

1. Introduction

Some of the ternary compounds existing in the cerium–nickel–tin system exhibit interesting physical properties. Previous studies have shown that $CeNiSn_2$ undergoes two antiferromagnetic phase transitions at $T_N^1 = 3.9$ K and $T_N^2 = 3.2$ K [1] and CeNiSn is a valence-fluctuating system with a very narrow pseudogap exhibiting semiconducting behaviour below 6 K [2], whereas $CeNi_2Sn_2$ can be classified as a heavy fermion antiferromagnet [3]. These various physical behaviours lead us to the search for new ternary stannides containing cerium and nickel.

During our investigation of the cerium–nickel–tin system, we have prepared the stannide Ce_2Ni_2Sn for the first time. It is worthwhile noting that other intermetallic compounds Ce_2Ni_2X have been previously reported: Ce_2Ni_2Al and Ce_2Ni_2Ga which crystallize in the orthorhombic structure related to the W_2CoB_2 or Mo_2NiB_2 types [4] whereas Ce_2Ni_2In adopts, as for U_2Ni_2In and U_2Ni_2Sn, the tetragonal ordered version of the U_3Si_2-type structure [5–7]. These two structure types are built by linkage of two different prisms: the $[Ce_8Ni_2]$ double trigonal prisms and the more or less deformed $[Ce_8X]$ tetragonal prisms.

We have investigated the crystal structure of Ce_2Ni_2Sn by X-ray diffractometry on a single crystal. In this paper, we discuss the structural properties of this ternary stannide by comparison with those of CeNiSn. Also, the magnetic and electrical properties of Ce_2Ni_2Sn are presented and compared with those observed for other stannides such as $CeNiSn_2$, $CeNi_2Sn_2$ and CeNiSn.

2. Experimental procedure

The samples Ce_2Ni_2Sn were obtained by melting of the constituent elements (all with stated purities above 99.9%) in an induction levitation furnace under a purified argon atmosphere. Then, the samples were sealed in an evacuated quartz tube and annealed for two weeks at 800 °C.

Microprobe analysis was used to check both the homogeneity and the composition of the obtained samples. The analysis was based on the measurements of the Ce $L\alpha_1$, Ni $K\alpha_1$ and Sn $L\alpha_1$ X-ray emission lines, which were compared with those obtained for CeNiSn used as a reference. The elemental analysis of Ce_2Ni_2Sn sample gives the following experimental atomic percentages: Ce, 39.1(6)%; Ni, 40.9(6)%; Sn, 20.0(5)%. These are close to those calculated for the ideal composition (Ce, 40%; Ni, 40%; Sn, 20%).

* Corresponding author.

SSDI 0925-8388(94)01397-7

The sample was characterized through the X-ray powder patterns collected using a Philips PW 1050 diffractometer with a diffracted beam graphite monochromator and Cu Kα radiation. The peak position determinations were carried out on pressed sample data, using a local decomposition program and a pseudo-Voigt profile function, and corrected with silicon as external standard (NIST SRM 640 b). Intensities of the diffraction lines were obtained from I_0 values of a Rietveld refinement on a sieved powder diffractogram. Single-crystal intensity data for Ce_2Ni_2Sn were measured on an Enraf-Nonius CAD-4 four-circle diffractometer with graphite-monochromated Mo Kα radiation and a scintillation counter with pulse height discrimination. The background was determined at both ends of each θ–2θ scan.

Magnetization measurements were carried out between 2 K and 300 K using both a pendulum susceptometer and a superconducting quantum interference device magnetometer. The electrical properties were investigated above 1.8 K by resistivity measurements using a four-probe d.c. technique.

3. Results and discussion

3.1. Crystal structure

The X-ray powder data of Ce_2Ni_2Sn stannide, given in Table 1, can be indexed on the basis of a centred orthorhombic unit cell having the following parameters: $a = 0.439\ 36(9)$ nm, $b = 0.573\ 96(9)$ nm and $c = 0.859\ 67(13)$ nm.

A single crystal of Ce_2Ni_2Sn was isolated by mechanical fragmentation from the annealed sample. An investigation by X-ray photographic techniques confirms the orthorhombic symmetry with the Laue group *mmm*. Systematic extinctions are observed for *hkl* with $h+k+l \neq 2n$ leading to four possible space groups: *Immm*, *Imm*2, *I*222, and $I2_12_12_1$. The intensities of 3429 reflections were measured in the reciprocal space corresponding to $-8 \leq h \leq 8$, $-11 \leq k \leq 11$ and $-16 \leq l \leq 16$. After Lorentz and polarization corrections, and application of a first absorption correction using transmission factor T calculations with crystal shape and size ($0.057 < T < 0.196$), these data lead to 472 reflections with $F_0^2 > 3\sigma(F_0^2)$ and to an internal inconsistency index value $R_{INT} = 0.055$.

The crystal structure of Ce_2Ni_2Sn was solved on the basis of the *Immm* group by Patterson function deconvolution with the heavy atom method leading to the position of the Ce atoms. Sn and Ni sites were obtained by successive difference Fourier syntheses. At this stage, with the isotropic model obtained ($R = 0.065$), a second absorption correction was performed with the program ABSORB [10] leading to $R_{INT} = 0.029$. Anisotropic temperature factors were applied to all the atoms. Using a weighting scheme $w = [\sigma(F_0)]^{-2}$ and an empirical isotropic extinction parameter, the refinement converges well and leads to final values of $R = 0.023$ and $R_w = 0.034$. The atomic scattering factors for neutral atoms and anomalous corrections were taken from Ref. [11]. Calculations for the structural analysis were performed using the program SHELX 76 [12]. The final structural parameters and the interatomic distances are listed in Tables 2 and 3 respectively for Ce_2Ni_2Sn.

A partial (001) projection of the structure of Ce_2Ni_2Sn is drawn in Fig. 1. This stannide is isotropic to other ternary compounds such as Ce_2Ni_2Al and Ce_2Ni_2Ga [4]. The structure is characterized by Sn atoms or Ni–Ni pairs occupying the [Ce_8] deformed double trigonal prisms (Fig. 2). The deformation of the Ni-centred trigonal prisms is observed in many ternary compounds such as Gd_3NiSi_2 [13] and can be explained by looking

Table 1
X-ray powder data of Ce_2Ni_2Sn

$2\theta_{obs}$	$100I/I_0$	d_{obs}	h	k	l	$2\theta_{cal} - 2\theta_{obs}$
22.685	5	3.917	1	0	1	0.026
25.501	9	3.490	1	1	0	0.010
31.144	17	2.869	0	2	0	−0.004
33.028	100	2.710	1	1	2	0.014
34.955	30	2.565	0	1	3	0.015
37.434	10	2.401	1	0	3	0.005
37.655	11	2.387	0	2	2	0.003
38.892	43	2.314	1	2	1	−0.004
41.040	23	2.197	2	0	0	0.014
41.983	12	2.150	0	0	4	0.023
52.095	4	1.754	1	3	0	0.003
52.401	9	1.745	2	2	0	0.009
53.218	2	1.720	0	2	4	−0.015
54.999	16	1.668	2	1	3	0.003
55.729	2	1.648	0	1	5	0.040
56.640	12	1.624	1	3	2	−0.013
56.951	6	1.616	2	2	2	−0.028
57.519	6	1.601	1	0	5	−0.004
57.927	10	1.591	0	3	3	−0.018
60.158	7	1.537	2	0	4	0.029
64.906	6	1.4355	0	4	0	0.030
65.078	2	1.4321	0	0	6	−0.034
66.878	21	1.3979	1	2	5	−0.018
69.750	12	1.3472	3	1	2	−0.021
			1	4	1	0.001
73.427	16	1.2885	2	3	3	−0.008

$M(20) = 53.5$ is the Wolff criterion [8]; $F(25) = 38.6$ (0.0151, 43) is the Smith and Snyder criterion [9].

Table 2
Atomic coordinates and equivalent thermal parameters for Ce_2Ni_2Sn

Atom	Site	x	y	z	B_{eq} (10^{-2} nm^2)
Ce	4j	1/2	0	0.2969(1)	0.79(1)
Ni	4h	0	0.2165(2)	1/2	1.18(2)
Sn	2a	0	0	0	0.71(1)

Table 3
Interatomic distances (nanometres) in Ce_2Ni_2Sn

Ce–Ce	0.3491(1)	Sn–4Ce	0.3359(1)
–4Ce	0.3703(1)	–4Ce	0.3368(1)
–2Ce	0.4394(1)		
		Sn–4Ni	0.2734(1)
Ce–2Sn	0.3359(1)		
–2Sn	0.3368(1)	Ni–2Ce	0.3027(1)
		–4Ce	0.3069(1)
		Ni–2Sn	0.2734(1)
Ce–2Ni	0.3027(1)	Ni–Ni	0.2485(2)
–4Ni	0.3069(1)		

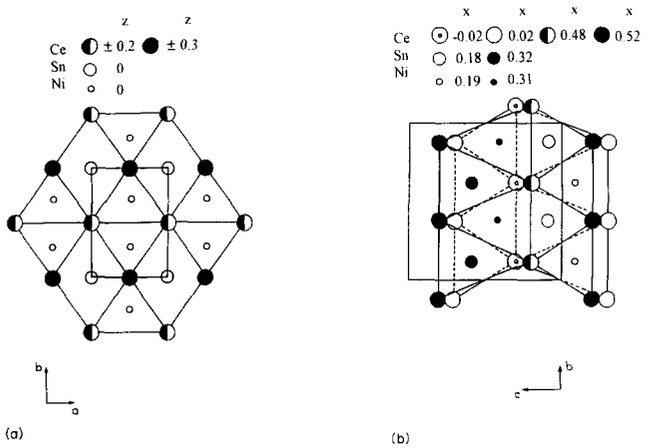

Fig. 1. (a) Partial projection of the crystal structure of Ce_2Ni_2Sn ($-0.3 \leq z \leq 0.3$) on the (001) plane; (b) partial projection of the crystal structure of CeNiSn ($-0.02 \leq x \leq 0.52$) on the (100) plane.

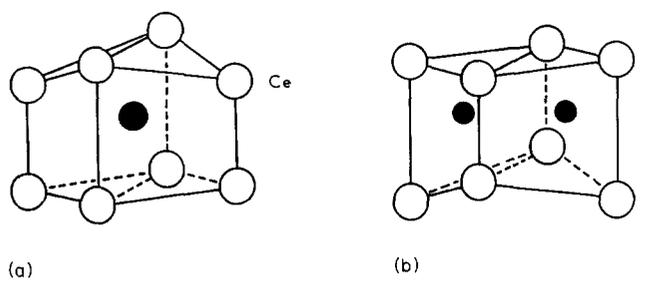

Fig. 2. Double trigonal prism [Ce_8] surrounding (a) a tin atom and (b) a nickel–nickel pair.

on the relative dimensions of such a prism in the RENi (RE = rare earth) binary compounds having the orthorhombic CrB or FeB type [14]. The Ni atoms occupy a compressed trigonal prism where the ratio of the height to the width of the prisms is less than 0.95. This observation can be related to the occurrence of the deformation of the double trigonal prism [Ce_8Ni_2] as shown in Fig. 2(b). On the contrary, in the Ce_2Ni_2Sn compound the Sn atoms are centred on the rectangular face shared by the two deformed trigonal prisms formed by Ce atoms (Fig. 2(a)). It is worthwhile noting that the volumes of the [Ce_8Sn] and [Ce_8Ni_2] prisms have the same value of 0.0541 nm^3.

In the ternary stannide CeNiSn crystallizing in the orthorhombic ϵ-TiNiSi-type structure, Sn and Ni atoms occupy a similar distorted trigonal prism [Ce_6] (Fig. 1(b)) [15]. In this arrangement, the –Ni–Sn–Ni–Sn– sublattice consists of zigzag chains running along the *b* axis. The change in stoichiometry from CeNiSn to Ce_2Ni_2Sn involves Sn atoms located inside [Ce_6] prisms in CeNiSn occupying the site at the centre of the rectangular face sharing two [Ce_6] prisms in Ce_2Ni_2Sn. The latter prisms form in the Ce_2Ni_2Sn compound the [Ce_8Sn] unit. It is worthwhile noting that the [Ce_6Ni] trigonal prisms are less deformed in Ce_2Ni_2Sn than in CeNiSn. This arises from the decrease in the tin content which leads to a reduction in the compression effect.

The crystal structure of Ce_2Ni_2Sn can be also described by a stacking of atomic planes perpendicular to the *c* axis: one containing Ni and Sn atoms and the other forming a 'wavy plane' of Ce atoms. A similar stacking can be considered to describe the crystal structure of the stannide U_2Ni_2Sn which crystallizes in the ordered tetragonal version of the U_3Si_2 type [6,16]. However, in the last case, the U atoms form an 'ideal' plane perpendicular to the *c* axis.

In Ce_2Ni_2Sn, the Ce atoms form a three-dimensional network (Fig. 1(a)). Each Ce atom is surrounded by seven neighbours: six in the basal plane (*a*–*b*) and one above it along the *c* axis (Table 3). Five of these Ce–Ce distances (0.3491 nm, four of 0.3703 nm) are clearly shorter than those found in CeNiSn where the average Ce–Ce bond length is equal to 0.382 nm [15]. All the Ce–Sn distances occurring in Ce_2Ni_2Sn are longer than the Ce–Ni distances in agreement with the values of the metallic radius of Sn and Ni ($r_{Sn} = 0.1623$ nm > $r_{Ni} = 0.1246$ nm). The Ce–Sn distances are larger than those observed in $CeSn_3$ (0.3339 nm) which is considered to be a typical intermediate valence compound [17]. Also, the Ce–Ni spacings in Ce_2Ni_2Sn are comparable with the shortest distance existing in CeNiSn (0.3064 nm).

3.2. Magnetic and electrical properties

Fig. 3 displays the reciprocal magnetic susceptibility χ_m^{-1} of Ce_2Ni_2Sn as a function of temperature in the range from 4.2 K to 290 K. Above 120 K, $\chi_m^{-1} = f(T)$ follows a Curie–Weiss law, leading to an effective magnetic moment of $2.42\mu_B$ (Ce atom)$^{-1}$. This value is slightly lower than that calculated for a free Ce^{3+} ion (2.54 μ_B). At lower temperatures ($T < 120$ K), χ_m increases more rapidly with decreasing temperature: this is probably due to the influence of the crystal field effect. An extrapolation of the $\chi_m^{-1} = f(T)$ curve for $T \geq 120$ K leads to a negative value for the paramagnetic Curie temperature ($\theta_p = -68$ K). This large negative

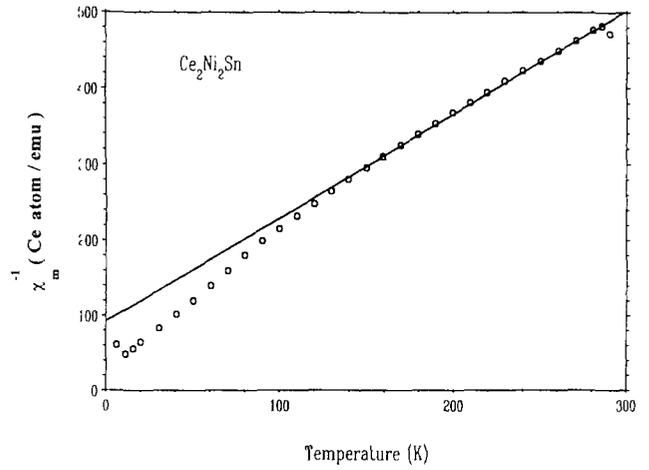

Fig. 3. Temperature dependence of the reciprocal magnetic susceptibility of Ce_2Ni_2Sn: —, Curie–Weiss law.

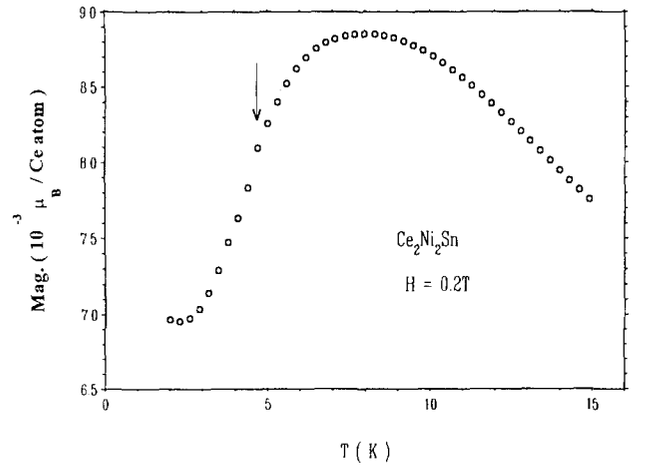

Fig. 4. Temperature dependence of the magnetization of Ce_2Ni_2Sn measured under an applied field $H=0.2$ T (the arrow indicates the Néel temperature).

value is a signature of a strong negative interaction between the spins of both 4f and conduction electrons associated with the Kondo effect.

Fig. 4 shows the thermal dependence of the magnetization of Ce_2Ni_2Sn measured under an applied field of 0.2 T. This curve reveals a broad maximum around 8 K, followed by a sharp drop at lower temperatures, suggesting the occurrence of an antiferromagnetic phase transition. The Néel temperature T_N, determined from the inflection point of the magnetization curve, is equal to 4.7 K. The magnetic behaviour of Ce_2Ni_2Sn is characteristic of a magnetically ordered heavy electron system such as U_2Zn_{17} [18]. The broad maximum near 8 K is therefore attributed to spin fluctuations arising from the Kondo effect. The magnetic properties of Ce_2Ni_2Sn appear to be governed by a strong competition between the Kondo interactions and the Ruderman–Kittel–Kasuya–Yoshida (RKKY) magnetic interactions. $T_K=8$ K is the estimated Kondo temperature whereas the magnetic ordering temperature is lower: $T_N=4.7$ K. This last temperature is higher than that observed for other cerium- and nickel-based stannides, for instance $CeNi_2Sn_2$ ($T_N=1.8$ K) [3].

The field dependence of the magnetization of Ce_2Ni_2Sn at $T=2$ K under external fields H up to 5 T is depicted in Fig. 5. This magnetic isotherm is linear with H down to 2.8 T but a positive curvature increases progressively with rising field. This behaviour which is suggestive of some kind of metamagnetism could be associated with the antiferromagnetic ordering of Ce_2Ni_2Sn.

The thermal dependence of the reduced electrical resistivity of Ce_2Ni_2Sn exhibits some characteristics of the magnetically ordered Kondo systems (Fig. 6): (i) a strong decrease below 4.7 K associated with the occurrence of the magnetic ordering; (ii) a pronounced

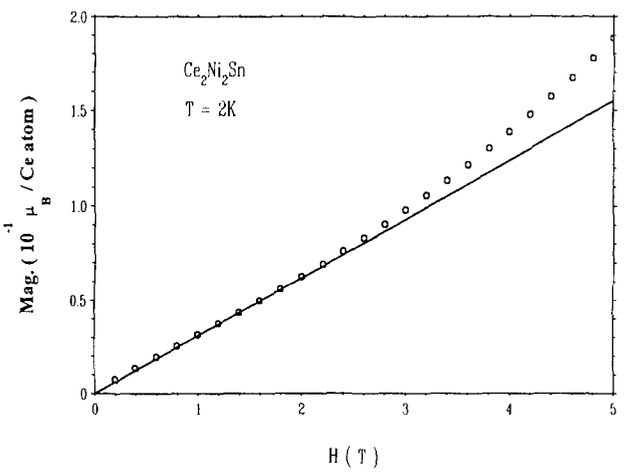

Fig. 5. Magnetization vs. applied field for Ce_2Ni_2Sn at 2 K.

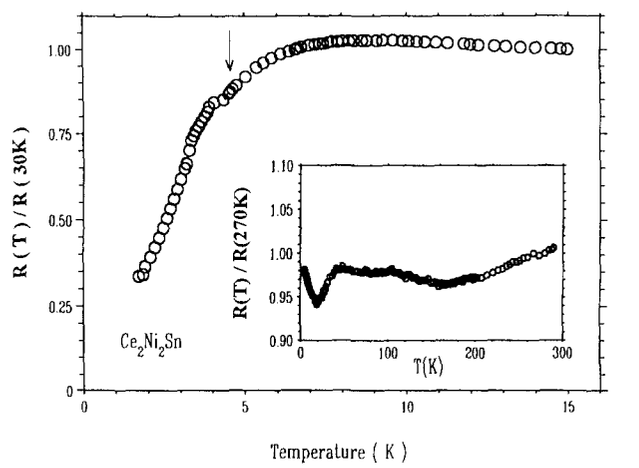

Fig. 6. Temperature dependence of the reduced electrical resistivity of Ce_2Ni_2Sn between 1.8 K and 15 K (the arrow indicates the Néel temperature). The resistivity vs. temperature for 4.2 K $\leq T \leq$ 270 K is also shown.

minimum at about 19 K bordered by two maxima appearing near 8 K and 40 K; (iii) finally a rather flat resistivity between 40 K and 270 K. It is interesting to take notice that, at low temperatures, $CeNi_2Sn_2$ displays a similar behaviour: a minimum at about 30 K and then a maximum at 8 K [19]. This last maximum has been explained as being the signature of the Kondo temperature. In the case of Ce_2Ni_2Sn, the occurrence of the maximum near 8–9 K could be associated also with the presence of the Kondo fluctuations. It is worthwhile noting that the appearance of the magnetic ordering is accompanied by a strong decrease in the electrical resistivity ($\rho(1.7\ K)/\rho(8\ K) \approx 0.3$) showing that the magnetic scattering is important in Ce_2Ni_2Sn.

The study of magnetic and electrical properties of Ce_2Ni_2Sn indicates the presence of the Kondo effects with $T_K = 8$ K. This comment can be made for other ternary stannides existing in the cerium–nickel–tin system since for instance the T_K value of $CeNi_2Sn_2$ is estimated to be 7.5 K from electrical resistivity measurements on single crystal [20] or 10 K from specific heat measurements [3].

4. Conclusion

The new ternary stannide Ce_2Ni_2Sn crystallizes in the orthorhombic structure deriving from the W_2CoB_2 type as Ce_2Ni_2Al or Ce_2Ni_2Ga. This stannide exhibits the behaviour of a magnetically ordered Kondo system. Its Néel temperature $T_N = 4.7$ K is greater than that determined for other stannides containing cerium and nickel: $CeNi_2Sn_2$ ($T_N = 1.8$ K) and $CeNiSn_2$ ($T_N^1 = 3.9$ K and $T_N^2 = 3.2$ K) [1,3]. Specific heat measurements are now in progress in order to examine whether the competition between Kondo and RKKY magnetic interactions leads to an enhancement of the electronic specific heat term γ.

References

[1] V.K. Pecharsky, K.A. Gschneidner, Jr., and L.L. Miller, *Phys. Rev. B, 43* (1991) 10906.
[2] T. Takabatake, F. Teshima, H. Fujii, S. Nishigori, T. Suzuki, T. Fujita, Y. Yamaguchi, J. Sakurai and D. Jaccard, *Phys. Rev. B, 41* (1990) 9607.
[3] W.P. Beyermann, M.F. Hundley, P.C. Canfield, J.D. Thompson, M. Latroche, C. Godart, M. Selsane, Z. Fisk and J.L. Smith, *Phys. Rev. B, 43* (1991) 13130.
[4] V.A. Romaka, Yu.N. Grin, Ya.P. Yarmolyuk, O.S. Zarechnyuk and R.V. Skolozdra, *Fiz. Met. Metalloved., 54* (1982) 691.
[5] Ya.M. Kalychak, V.I. Zaremba, V.M. Baranyak, P.Yu. Zavalii, V.A. Bruskov, L.V. Sysa and O.V. Dmytrakh, *Izv. Akad. Nauk SSSR, Neorg. Mater., 26* (1990) 94.
[6] F. Mirambet, B. Chevalier, L. Fournès, P. Gravereau and J. Etourneau, *J. Alloys Compd., 203* (1994) 29.
[7] M.N. Peron, Y. Kergadallan, J. Rebizant, D. Meyer, J.M. Winnand, S. Zwirner, L. Havela, H. Nakotte, J.C. Spirlet, G.M. Kalvius, E. Colineau, J.L. Oddou, C. Jeandey and J.P. Sanchez, *J. Alloys Compd., 201* (1993) 203.
[8] P.M. de Wolff, *J. Appl. Crystallogr., 1* (1968) 108.
[9] G.S. Smith and R.L. Snyder, *J. Appl. Crystallogr., 12* (1979) 60.
[10] F. Ugozzoli, *Comput. Chem., 11* (1987) 109.
[11] J.A. Ibers and W.C. Hamilton (eds.), *International Tables for X-ray Crystallography*, Vol. IV, Kynoch, Birmingham, 1974.
[12] G.M. Sheldrick, SHELX 76, *Program for Crystal Structure Determination*, University of Cambridge, 1976.
[13] K. Klepp and E. Parthé, *Acta Crystallogr. B, 37* (1981) 1500.
[14] A.E. Dwight, R.A. Conner, Jr., and J.W. Downey, *Acta Crystallogr., 18* (1965) 835.
[15] I. Higashi, K. Kobayashi, T. Takabatake and M. Kasaya, *J. Alloys Compd., 193* (1993) 300.
[16] F. Bourée, B. Chevalier, L. Fournès, F. Mirambet, T. Roisnel, V.H. Tran and Z. Zolnierek, *J. Magn. Magn. Mater.*, to be published.
[17] J. Lawrence, *Phys. Rev. B, 20* (1979) 3770.
[18] H.R. Ott, H. Rudiger, P. Delsing and Z. Fisk, *Phys. Rev. Lett., 52* (1984) 1551.
[19] K. Kaczmarska, J. Pierre, A. Slebarski and R.V. Skolozdra, *J. Alloys Compd., 196* (1993) 165.
[20] T. Takabatake, F. Teshima, H. Fujii, S. Nishigori, T. Suzuki, T. Fujita, Y. Yamaguchi and J. Sakurai, *J. Magn. Magn. Mater., 90–91* (1990) 474.